JOURNAL OF APPLIED ELECTROCHEMISTRY 15 (1985) 459–468

Behaviour of Li_4SiO_4 and its solid solutions during d.c. and a.c. measurements

K. JACKOWSKA*, A. R. WEST

University of Aberdeen, Department of Chemistry, Meston Walk, Aberdeen, AB9 2UE, UK

Received 26 June 1984; revised 10 September 1984

Pellets of three compositions, Li_4SiO_4, $Li_{4.3}(Si_{0.7}Al_{0.3})O_4$ and $(Li_{3.82}Al_{0.06})SiO_4$ have been subjected to d.c. and a.c. measurements over a range of temperatures and voltages using gold electrodes in a symmetrical cell arrangement. At low temperatures, $\lesssim 200^\circ$ C, the electrode–electrolyte interfaces behave as a simple double layer capacitor but at higher temperatures complex behaviour, associated with electrochemical decomposition of the pellets, is observed.

1. Introduction

The a.c. conductivity measurements on solid electrolytes are frequently made using gold electrodes which are assumed to be blocking at small applied voltages. It has recently been shown, however, that a variety of ionic solids, including Li_4SiO_4, Li_2SiO_3 and, to a certain extent Na β-alumina, undergo electrochemical decomposition at high temperatures e.g. $\gtrsim 400^\circ$ C with relatively small applied voltages, e.g. 0.1 to 0.5 V [1–3]. The products of decomposition are solids that remain in the vicinity of the electrode–electrolyte interface and may subsequently rereact when the cells are allowed to discharge. Although gold electrodes were used in the construction of the cells, it was shown [2–4] that the gold took no part in the overall operation of the cells and other electrode materials could conceivably be used. These all-solid state, high temperature cells have various possible applications which include thermal batteries, high temperature constant voltage sources and thermal switching devices. They should also lend themselves to miniaturization using thin film techniques.

In this paper, we report the results of combined a.c. and d.c. measurements on polycrystalline Li_4SiO_4 and two Li_4SiO_4-based solid solutions that have enhanced conductivity [5]. The objective has been to gain an increased understanding of the processes that occur under the action of an applied voltage.

The solid solutions chosen for study both have the Li_4SiO_4 structure but lie on different joins in the system Li_2O–Al_2O_3–SiO_2 [5]. The interstitial solid solutions lie on the join Li_4SiO_4–Li_5AlO_4 and have general formula $Li_{4+x}(Si_{1-x}Al_x)O_4$; for this study, a composition with $x = 0.30$ was chosen. The vacancy solid solutions lie on the join Li_4SiO_4-$LiAlSiO_4$ with general formula $(Li_{4-3x}Al_x)SiO_4$; composition $x = 0.06$ was selected.

2. Experimental details

Li_4SiO_4 and its solid solutions $Li_{4.3}(Si_{0.7}Al_{0.3})O_4$ and $(Li_{3.82}Al_{0.06})SiO_4$ were synthesized by solid state reaction of Li_2CO_3, SiO_2 and Al_2O_3 in gold foil boats in electric muffle furnaces at temperatures increasing from 600 to 900° C [5]. Completeness of reaction was checked by X-ray powder diffraction using a Hägg Guinier focusing camera, Cu$K\alpha_1$ radiation. Pellets were cold-pressed at 2 tons cm^{-2} and sintered at 1000° C for 2 h in order to increase their mechanical strength, reduce porosity and improve the intergranular contact. Final pellet porosities were ~ 15%. Gold foil electrodes were attached to opposite pellet faces using Engelhard gold paste; the pellets were then gradually heated to 500° C and held at that temperature for 30 min in order to decompose the organogold

* Permanent address: Laboratory of Electrochemistry, Department of Chemistry, University of Warsaw, Poland.

0021–891X/85 $03.00 + .12

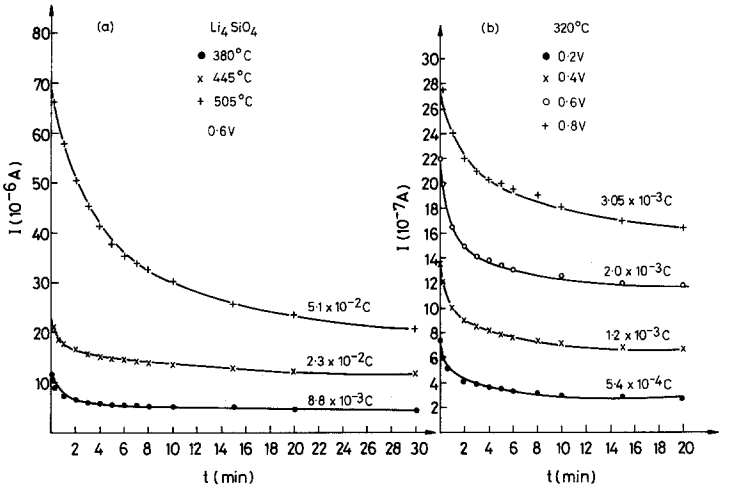

Fig. 1. Li_4SiO_4, pellet density 1.75 g cm^{-3}; current versus time behaviour on charging as a function of (a) temperature and (b) voltage.

paste and harden the residue. Previous experiments had shown that either gold foil or evaporated gold electrodes could also be used [2–4] and similar results obtained. Here it was most convenient to use electrodes made from gold paste. The pellets with electrodes attached to platinum wire leads, were placed inside a vertical tube furnace whose temperature was controlled to ± 1° C.

The d.c. charging and discharging experiments were carried out by means of a simple electrical set-up in which a constant voltage source was used to apply a voltage, in the range 0.1 to 1.0 V, across the pellet. This applied voltage was checked with a digital voltmeter. The current passing through the cell was measured by recording the potential drop across a standard resistor in series with the cell, using a Chessell millivoltmeter/chart recorder. The standard resistors were carefully chosen so as to permit measurements on cells containing pellets of low conductivity (at certain temperatures). In order to discharge the cells, the d.c. power source was removed from the circuit and the leads to the recorder reversed. The total charge passed was determined from the area under the I versus t curves.

The a.c. impedance measurements were made on cells of similar design using a Solartron 1172 frequency analyser operating over the frequency range 10^{-3} to 10^4 Hz. For these measurements, the cell was connected in series with a standard resistor and a constant voltage, usually 0.1 V, applied across them. The voltage across the cell was not known accurately, but was less than the nominal applied voltage and varied with frequency as the cell impedance varied. All measurements were carried out in air.

3. Results and discussion

3.1. *Charging and discharging experiments*

Pellets of three different compositions were used for the charging–discharging experiments:

(i) Li_4SiO_4
(ii) $Li_{4.3}(Si_{0.7}Al_{0.3})O_4$
(iii) $(Li_{3.82}Al_{0.06})SiO_4$

The temperatures used were in the range 245 to 500° C for (i) and 100 to 380° C for (ii, iii) with applied voltages in the range 0.1 to 1.0 V. Typical charging curves of I versus t are given in Figs. 1–3 for (a) constant voltage at a series of temperatures, and (b) constant temperature for a series of voltages. Charging times were generally either 30 or 60 min and the total charges passed, determined from the areas under the curves, are indicated in Figs. 1 and 2. Significant increases in the charging currents were found with both increasing temperature and increasing applied voltage. For pellets (i) and (iii), the charging current tended towards a steady rate value for times $\gtrsim$ 20 min, suggesting that an electrode reaction was taking place at the electrode–electrolyte interface. A similar effect was observed with pellet (ii) at high temperatures, but at lower temperatures, the charging current gradually decreased with time.

Similar curves to Figs. 1–3 were obtained on subsequent discharge of the cells, although in these cases, the discharge currents eventually

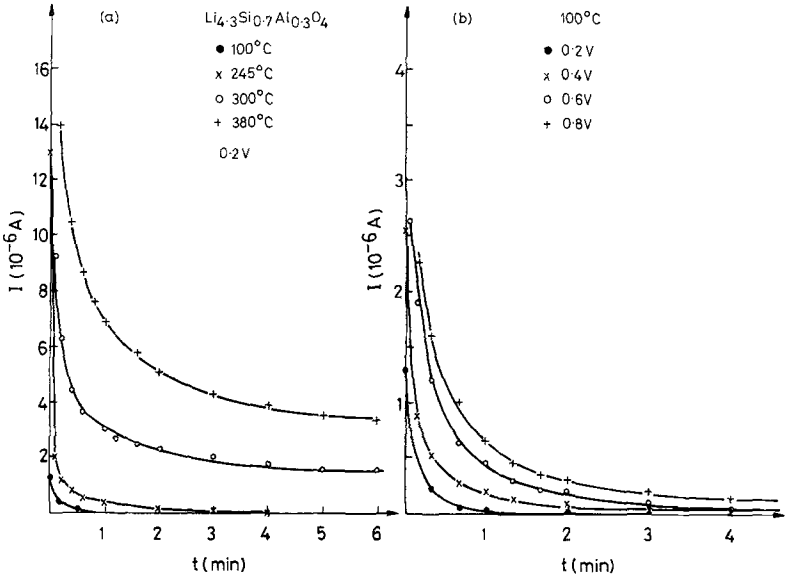

Fig. 2. $Li_{4,3}(Si_{0,7}Al_{0,3})O_4$, pellet density 1.63 g cm^{-3}; current versus time behaviour on charging as a function of (a) temperature and (b) voltage.

decreased to zero. These results (not shown) together with those for charging were used to calculate the amount of charge that was effectively lost during charging, and not recovered on discharging, as follows:

$$\text{loss}, L = \left(1 - \frac{Q_{\text{discharge}}}{Q_{\text{charge}}}\right) \times 100\% \quad (1)$$

The values of $Q_{\text{discharge}}$ and Q_{charge} were determined after fixed times: (i) 30 min, (iii) 60 min and (ii) after the current had decreased to 1% of its initial value, generally a few minutes. Values of L as a function of temperature and voltage are given in Table 1.

These results, Figs. 1–3, Table 1, indicate that two types of process occur during the charging experiments. At low temperatures, $\lesssim 200°$ C, as seen in (ii), the losses were small and the overall amounts of charge that were stored and recovered, 10^{-4} to 10^{-5} C, were also small, indicative of an essentially double layer capacitance behaviour.

At high temperatures, the Q values were

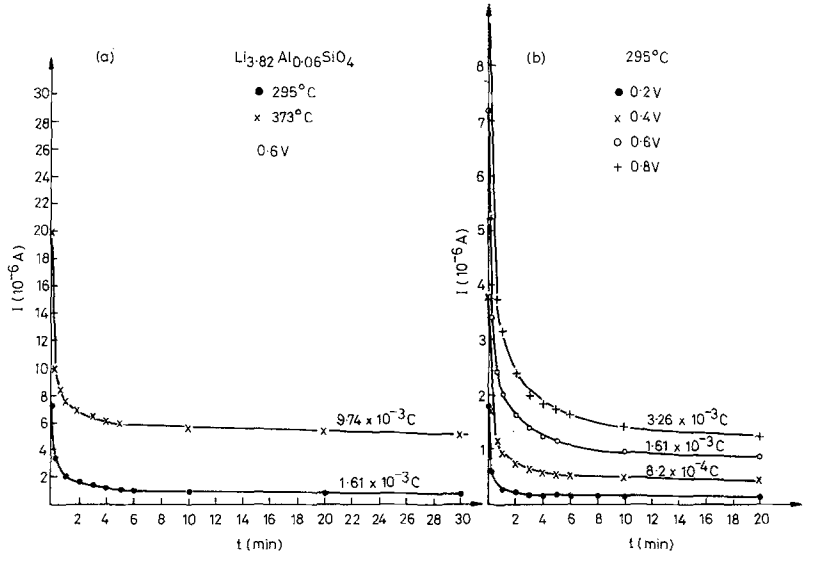

Fig. 3. $(Li_{3,82}Al_{0,06})SiO_4$, pellet density 1.71 g cm^{-3}, current versus time behaviour on charging as a function of (a) temperature and (b) voltage.

Table 1. Summary of charging–discharging experiments

Li_4SiO_4				$Li_{4.3}(Si_{0.7}Al_{0.3})O_4$				$(Li_{3.82}Al_{0.06})SiO_4$			
T° C	*Charging Voltage (V)*	*Average charge passed (C)*	*Loss L (%)*	*T° C*	*Charging voltage (V)*	*Average charge passed (C)*	*Loss L (%)*	*T° C*	*Charging voltage (V)*	*Average charge passed (C)*	*Loss L (%)*
245	0.2	$\sim 10^{-5}$	87	100	0.2	$\sim 10^{-5}$	0	150	0.2	$\sim 10^{-5}$	54
	0.4	$\sim 10^{-4}$	84		0.4	$\sim 10^{-5}$	1	200	0.2	$\sim 10^{-5}$	58
	0.6	$\sim 10^{-4}$	82		0.6	$\sim 10^{-5}$	10		0.4	$\sim 10^{-4}$	58
	0.8	$\sim 10^{-4}$	81		0.8	$\sim 10^{-4}$	7		0.6	$\sim 10^{-4}$	60
	1.0	$\sim 10^{-4}$	81	150	0.2	$\sim 10^{-5}$	0		0.8	$\sim 10^{-4}$	60
320	0.2	$\sim 10^{-4}$	74		0.4	$\sim 10^{-5}$	6	295	0.1	$\sim 10^{-4}$	70
	0.4	$\sim 10^{-3}$	77		0.6	$\sim 10^{-4}$	21		0.2	$\sim 10^{-4}$	70
	0.6	$\sim 10^{-3}$	82		0.8	$\sim 10^{-4}$	24		0.4	$\sim 10^{-4}$	70
	0.8	$\sim 10^{-3}$	83	196	0.1	$\sim 10^{-5}$	12		0.6	$\sim 10^{-3}$	64
	1.0	$\sim 10^{-3}$	84		0.2	$\sim 10^{-5}$	17		0.8	$\sim 10^{-3}$	83
381	0.2	$\sim 10^{-3}$	64		0.3	$\sim 10^{-4}$	18	373	0.1	$\sim 10^{-3}$	58
	0.4	$\sim 10^{-3}$	64		0.4	$\sim 10^{-4}$	17		0.2	$\sim 10^{-3}$	58
	0.6	$\sim 10^{-3}$	76		0.5	$\sim 10^{-4}$	18		0.4	$\sim 10^{-3}$	78
	0.8	$\sim 10^{-3}$	76	245	0.1	$\sim 10^{-5}$	35		0.6	$\sim 10^{-3}$	87
	1.0	$\sim 10^{-2}$	81		0.2	$\sim 10^{-5}$	56				
445	0.2	$\sim 10^{-2}$	75		0.3	$\sim 10^{-4}$	57				
	0.4	$\sim 10^{-2}$	77		0.4	$\sim 10^{-4}$	64				
	0.6	$\sim 10^{-2}$	81	300	0.1	$\sim 10^{-4}$	83				
	0.8	$\sim 10^{-2}$	84		0.2	$\sim 10^{-3}$	85				
	1.0	$\sim 10^{-2}$	86		0.3	$\sim 10^{-3}$	87				
505	0.2	$\sim 10^{-2}$	74		0.4	$\sim 10^{-3}$	84				
	0.4	$\sim 10^{-2}$	72		0.5	$\sim 10^{-3}$	85				
	0.6	$\sim 10^{-2}$	78	380	0.1	$\sim 10^{-3}$	81				
	0.8	$\sim 10^{-1}$	85		0.2	$\sim 10^{-3}$	90				
	1.0	$\sim 10^{-1}$	85		0.3	$\sim 10^{-3}$	80				
					0.4	$\sim 10^{-3}$	82				

generally several orders of magnitude larger, 10^{-1} to 10^{-3} C and the losses were much higher, only 10–30% of the charge being recoverable. These charge magnitudes are too high to be attributable to conventional double layer phenomena and are more consistent with the occurrence of electrochemical reactions at the electrode–electrolyte interfaces.

The occurrence of steady state currents after long times of charging may perhaps, at first sight, be attributable to electronic conduction or possibly, conduction by oxide ions. However, if this were the case, only small discharge currents would be possible, giving $Q_{\text{discharge}} \sim 10^{-4}$ to 10^{-5} C. Since the discharge currents were usually at least two orders of magnitude greater than these values, such effects cannot be of major significance in the present materials.

The results of Table 1 show that the losses, or cell efficiencies vary little with applied voltage, at least in the range 0.1 to 1.0 V and with temperature, at least in the range ~250 to 500° C.

The reactions that occur on charging cell (i) have been previously investigated [3] and lead to the formation of Li_2CO_3 and Li_2SiO_3 at the cathode and anode, respectively. X-ray powder diffraction of pellet surfaces before and after charging was carried out on the present Li_4SiO_4 samples and these same two crystalline phases were also detected in small amounts at the appropriate electrodes. The reactions by which these products form are possibly:

cathode:

$$2Li^+ + \tfrac{1}{2}O_2 + 2e \rightarrow Li_2O \text{ (electrochemical)} \quad (2a)$$

$$Li_2O + CO_2 \rightarrow Li_2CO_3 \text{ (chemical)} \quad (2b)$$

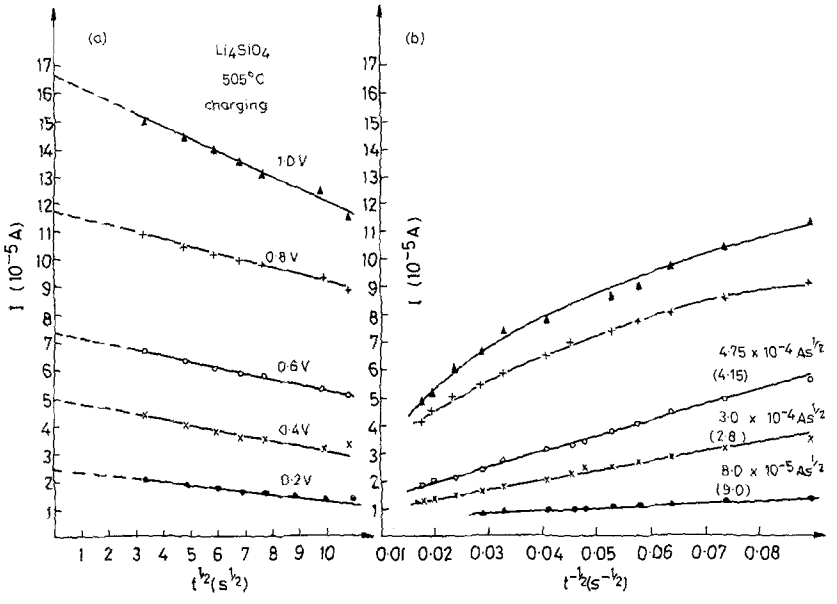

Fig. 4. Li_4SiO_4; (a) current versus time $^{\frac{1}{2}}$ and (b) current versus time$^{-\frac{1}{2}}$ dependance on charging at 505° C.

anode:

$$Li_4SiO_4 \rightarrow Li_2SiO_3 + \tfrac{1}{2}O_2 + 2Li^+ + 2e$$

(electrochemical) (3)

overall:

$$Li_4SiO_4 + CO_2 \rightarrow Li_2SiO_3 + Li_2CO_3 \quad (4)$$

The products obtained on charging pellets (ii) and (iii) were not identified and the role of Al^{3+} is at present not known.

3.2. *Analysis of current–time curves*

The current–time curves obtained on charging, Figs. 1–3 and discharging were clearly non-exponential. Since the current flow is attributed to transport of Li^+ ions through the bulk of the pellets, together with electrochemical reactions at the electrode–electrolyte interface and possible transport through the product layer(s), a diffusion-controlled behaviour might be anticipated. On application of a step potential to a previously equilibrated cell, the concentration of ions at the electrode–electrolyte interface changes abruptly; re-equilibration in the distribution of ions may then be reached by chemical diffusion. During electrolysis, concentration gradients of electroactive ions may also build up and diffusional transport may occur if the charge transfer reaction is rapid. For such diffusion-controlled phenomena, the current should depend linearly on the reciprocal of the square root of time with the constant of proportionality, K, being related to the diffusion coefficient, ie.

$$I = Kt^{-\frac{1}{2}} \quad (5)$$

This equation was found to be applicable to all three pellet materials over a wide range of conditions, Figs. 4–6. For Li_4SiO_4, Equation 5 held for a range of temperatures and times, Fig. 4b. Exceptions were for (a) short times, $\lesssim 3$ mins, Fig. 4a, for which the alternative equation:

$$I = Kt^{\frac{1}{2}} \quad (6)$$

was found, (b) high charging voltages at high temperatures, 0.8 and 1.0 V at 505° C and (c) long times of charging in which the current had reached a steady-state value:

$$I = I_{const} \quad (7)$$

For $Li_{4.3}(Si_{0.7}Al_{0.3})O_4$, (ii), Equation 5 was found to hold for times ranging from a few seconds to a few minutes, Fig. 5, for temperatures of 300° C and below. For longer times the current had decreased either to zero or to a constant value, Equation 7.

For $(Li_{3.82}Al_{0.06})SiO_4$, the results were more

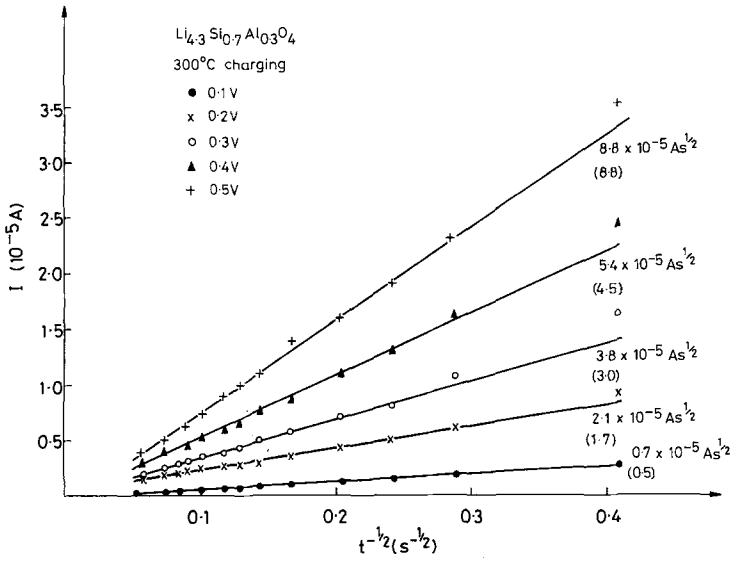

Fig. 5. $Li_{4\cdot3}(Si_{0\cdot7}Al_{0\cdot3})O_4$; current versus time$^{-\frac{1}{2}}$ dependance on charging at 300° C.

complicated and Equation 5 was found to be operative only at temperatures $>250°$ C, Fig. 6.

The slopes, K, of the graphs shown in Figs. 4b, 5 and 6 were determined and are indicated on the graphs, together with, in parentheses, the values for the corresponding discharge curves. Agreement between the two sets of K values is generally good. The slopes, K, should be related to the diffusion coefficient which is a temperature dependent parameter. The results clearly show that K also depends on voltage and hence the relation between K and the diffusion coefficient is not simple. Nevertheless, the frequent applicability of Equation 5 to the experimental results indicates a diffusion-controlled current flow mechanism.

3.3. *Low frequency a.c. impedance measurements*

The electrical properties of an ideal solid electrolyte can be represented by a simple equivalent circuit containing a bulk resistance, R_b, and geometric capacitance, C_g, in parallel. For polycrystalline electrolytes with blocking electrodes additional circuit elements representing grain boundary impedance and double layer capacitance must be included. The circuit becomes further complicated

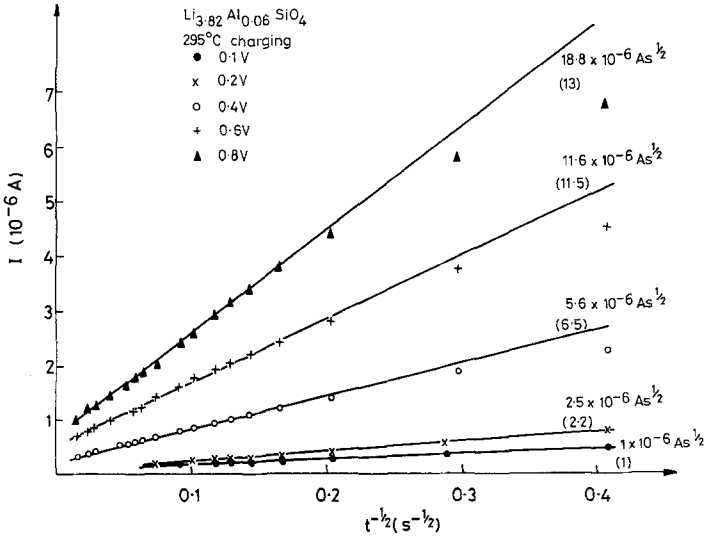

Fig. 6. $(Li_{3\cdot82}Al_{0\cdot06})SiO_4$; current versus time$^{-\frac{1}{2}}$ dependance on charging at 295° C.

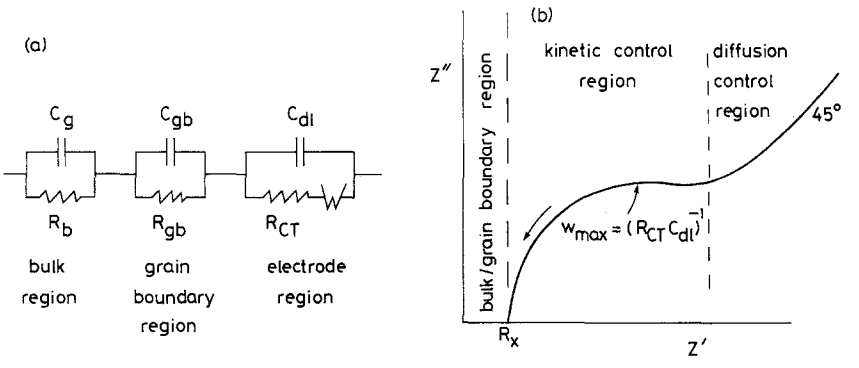

Fig. 7. (a) Equivalent circuit for an electrolyte cell that is undergoing electrode reactions. (b) Schematic complex impedance plot at low frequencies for (a).

when electrode reactions can occur, Fig. 7a. Then a charge transfer resistance, R_{CT} and a Warburg impedance, W, associated with diffusion controlled processes may also be introduced into the equivalent circuit. In practice, the charge transfer and diffusion controlled regions may not be well defined and the observed 'electrode' response in the complex impedance plane depends on the relative magnitudes of R_{CT} and W. If the electrode reactions are kinetically sluggish, a large R_{CT} will be present leading to an impedance plane plot dominated by a large semicircle. Conversely, if R_{CT} is small the semicircle associated with R_{CT} and C_{DL} will be small and a straight line of ideal slope 45°, associated with the Warburg impedance should dominate the complex impedance plane at low frequencies. A schematic response in which both R_{CT} and W are significant is shown in Fig. 7b.

The formation of product layer(s) at the electrode–electrolyte interface may cause additional complications and lead to extra RC elements in the equivalent circuit with associated semicircles in the complex impedance plane.

The a.c. impedance measurements were made on pellets of the same three compositions as used for the d.c. measurements and also at similar temperatures. Measurements were made over the frequency range 10^{-3} to 10^4 Hz with a nominal applied voltage of, usually, 0.1 V. However, as indicated in the Experimental section, the actual voltage dropped across the sample was smaller than the nominal applied value and varied with frequency. Nevertheless, the conditions under which the d.c. and a.c. measurements were carried out were sufficiently similar that the same phenomena should be observed in both.

Typical results are shown in Figs. 8–10 for

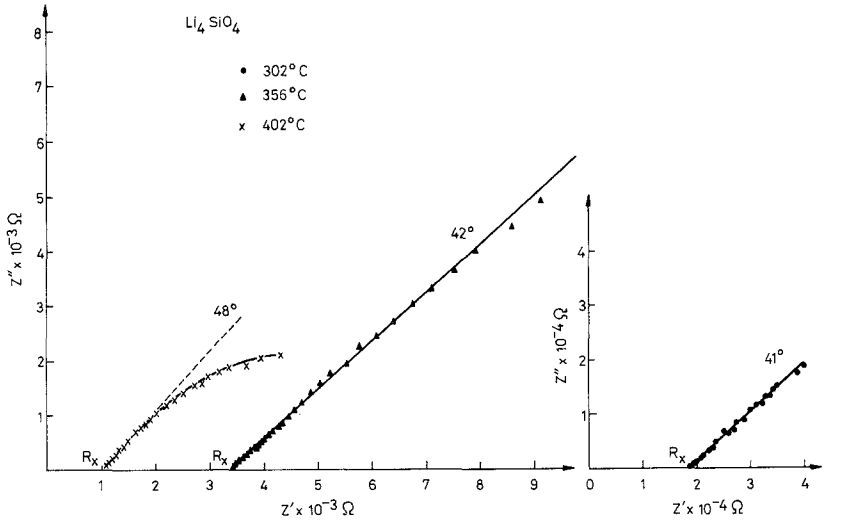

Fig. 8. Complex impedance plots, Li_4SiO_4, at various temperatures.

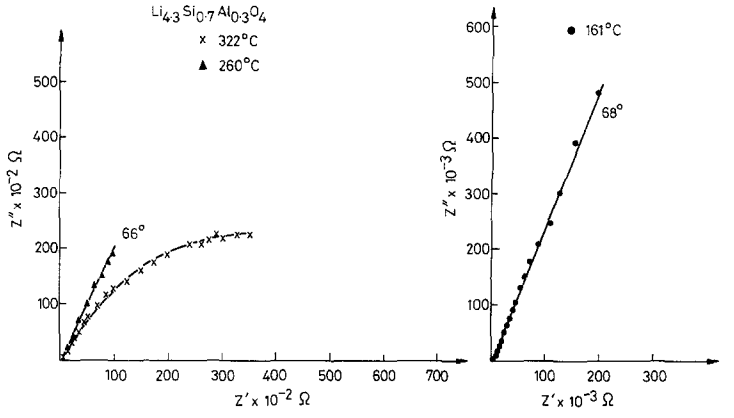

Fig. 9. Complex impedance plots, $Li_{4.3}(Si_{0.7}Al_{0.3})O_4$ at various temperatures.

pellets (i) to (iii), respectively. Values of the intercept, R_X on the real, Z' axis were converted to conductivity values and compared with the values obtained from frequency independent plateaux in log conductivity versus log frequency plots obtained at higher frequencies using admittance bridges [5]. These results, listed in Table 2, show good agreement usually and indicated that the resistance R_X represents the effective overall resistance of the pellet, especially at low temperatures, $\lesssim 300°$ C. At higher temperatures, discrepancies are seen between the two sets of results but, as described later, these values of R_X were found to be voltage dependent and cannot represent simply the pellet resistance.

The complex impedance plots, Figs. 8–10 show a variety of results but certain features are clear. At the lower temperatures, results approaching those expected for a 'blocking electrode spike' are seen. For example in Fig. 9, 161, 260° C; Fig. 10, 246, 316° C, straight lines of slope in the range 60 to 70° C are seen, which are somewhat deviated from the ideal value of 90° for a perfect double layer capacitance. These results are consistent with those obtained in the d.c. experiments which indicated essentially capacitance behaviour at low temperatures.

At higher temperatures, various combinations of a Warburg type response at $\sim 45°$ and a flattened semicircle are seen. The capacitance values calculated from the impedance and frequency of the semicircle maxima are in the range 10^{-4} to 10^{-3} F. These are 1 to 2 orders of magnitude larger than typical double layer values and several orders of magnitude larger than would be expected for the electrical response of a product layer(s). These results clearly indicate that electrode reactions are occurring and that the current flow is not simply diffusion controlled.

The difficulties associated with making a.c.

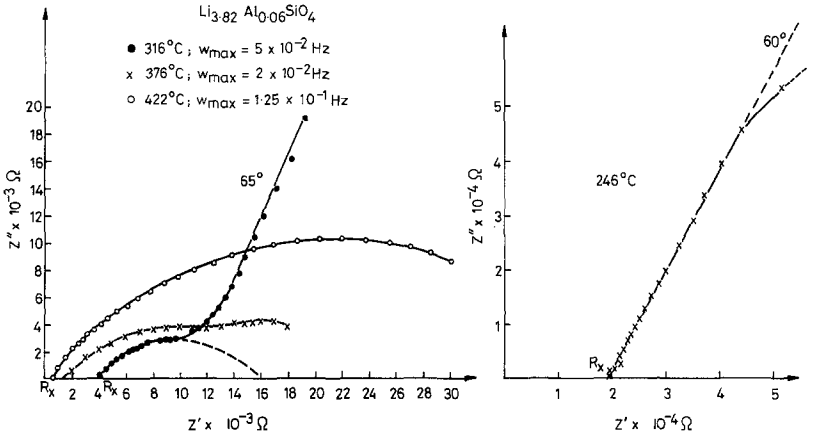

Fig. 10. Complex impedance plots, $(Li_{3.82}Al_{0.06})SiO_4$ at various temperatures.

Table 2. Conductivity values ($ohm^{-1}\ cm^{-1}$)

Li_4SiO_4			$Li_{4.3}(Si_{0.7}Al_{0.3})O_4$			$(Li_{3.82}Al_{0.06})SiO_4$		
$T°C$	σ (Bridge plateau value)	σ (Impedance R_X value)	$T(°C)$	σ (Bridge plateau value)	σ (Impedance R_X value)	$T(°C)$	σ (Bridge plateau value)	σ (Impedance R_X value)
302	1.96×10^{-5}	1.81×10^{-5}	161	6.91×10^{-5}	6.4×10^{-5}	210	2.56×10^{-6}	2.4×10^{-6}
356	9.44×10^{-5}	9.7×10^{-5}	210	2.41×10^{-4}	2.56×10^{-4}	264	1.69×10^{-5}	1.6×10^{-5}
402	3.39×10^{-4}	3.2×10^{-4}	260	7.83×10^{-4}	7.75×10^{-4}	316	8.46×10^{-5}	5.6×10^{-5}
			322	2.08×10^{-3}	3.4×10^{-3}	376	2.64×10^{-4}	2.0×10^{-4}
			379	4.35×10^{-3}	5.68×10^{-3}	422	6.6×10^{-4}	4.4×10^{-4}

impedance measurements on solid electrolytes under conditions where electrode reactions occur are further indicated in Fig. 11. A pellet of composition (iii) was subjected to three cycles of a.c. impedance measurements and the results are clearly different each time. The high frequency intercept, R_X, is essentially unchanged but a low frequency arc is obtained that grows in size with increasing time.

Results [4] that show the effect of varying the nominal applied voltage are given in Fig. 12 for a pellet of Li_4SiO_4 (i). Measurements were made on the same pellet, first at 0.05 V, then at 0.2 V and finally at 0.5 V. The results clearly show that the magnitude of the intercept R_X decreases with increasing voltage and indicate that, in these high temperature measurements, R_X does not represent the overall pellet resistance.

4. Conclusions

The a.c. and d.c. measurements show that at relatively low temperatures $\lesssim 200°$ C, the Li^+ ion conducting solid electrolyte Li_4SiO_4 and its solid solutions, with gold electrodes, behave effectively as double layer capacitors at low frequencies. At higher temperatures, reactions occur at the electrode–electrolyte interfaces which are associated with electrochemical decomposition of the pellets. This is shown by

(a) the large amounts of charge that can be stored and released
(b) the reduced efficiency of the charge storage process, as compared to the double layer capacitor behaviour
(c) the form of the current–time curves which indicate a diffusion controlled process
(d) the low frequency response in the complex impedance plane, which indicates a combination of a Warburg impedance and other effects associated with very large capacitance values, and
(e) time and voltage dependent response in the complex impedance plane at low frequencies.

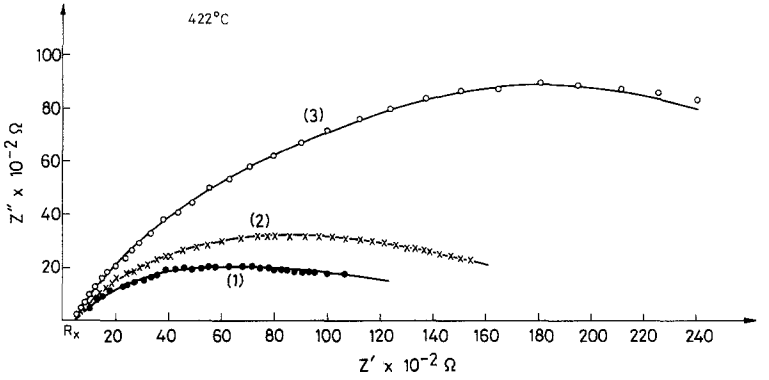

Fig. 11. Complex impedance plots, $(Li_{3.82}Al_{0.06})SiO_4$ at 422° C. Runs were made in seqence (1), (2), (3) on the same cell; run (2) was immediately after run (1); after (2), the cell was kept at 1.5×10^{-3} Hz for 12 h prior to run (3).

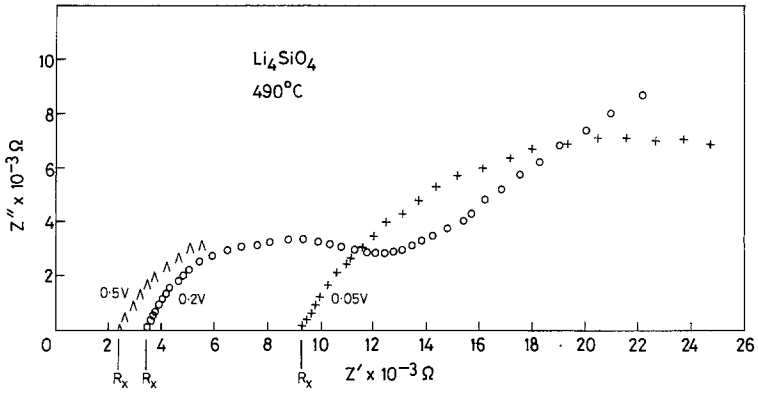

Fig. 12. Complex impedance plots, Li_4SiO_4; effect of increasing voltage. The same cell was used throughout.

Since these effects were observed at voltages as small as 50 and 100 mV, the results have wider implications for a.c. measurements on solid electrolytes at high temperatures.

Acknowledgements

A. R. West thanks the SERC for a research grant.

References

[1] J. M. Aceves, B. G. Cooksley and A. R. West, *J. Electroanal. Chem.* **90** (1978) 295.
[2] J. M. Aceves and A. R. West, *J. Appl. Electrochem.* **10** (1980) 379.
[3] *Idem, JCS Faraday I* 78 (1982) 2599.
[4] J. M. Aceves, PhD Thesis, University of Aberdeen (1980).
[5] K. Jackowska and A. R. West, *J. Mater. Sci.* 18 (1983) 2380.